Available online www.jsaer.com

***Journal of Scientific and Engineering Research*, 2018, 5(9):125-132**

Research Article

ISSN: 2394-2630
CODEN(USA): JSERBR

External Quantum Efficiency (EQE) and Internal Quantum Efficiency (IQE) in a 3D Cylindrical Modeling Study

Assane Diouf[1,2], Mahamadi Savadogo[3], Senghane Mbodji[1,2*]

[1]Research team in Renewable Energies, Materials and Laser of Department of Physics, Alioune DIOP University of Bambey, Bambey, Senegal
[2]Laboratory of Semiconductors and Solar Energy, Department of Physics, Faculty of Science and Technology, Cheikh Anta Diop University, Dakar, Senegal
[3]Laboratory of Thermal and Renewable Energies, Department of Physics, Unit of Training and Research in Pure and Applied Sciences, University of Ouagadougou Professeur Joseph KI-ZERBO, Burkina Faso

Abstract In this work, the cylindrical columnar grain model is used for the characterization of a polycrystalline silicon solar cell with an n+/p junction, under monochromatic illumination and operating in steady state condition. The Bessel functions and the dynamic velocity at the junction (S_f) are used to solve the continuity equation. In short circuit operating mode, expressions of minority carrier's density ($\delta_{sc}(r,z)$) and the photocurrent density (J_{SC}) are given. The expressions of external ($EQE(\lambda,r,Sgb)$) and internal ($IQE(\lambda,r,Sgb)$) quantum efficiencies are also given, as functions of grain radius (R), grain depth (z), and wavelength (λ) of the exciter light. On the basis of these expressions, effects of grain size and the grain boundaries recombination velocity on both external and internal quantum efficiencies are presented and analyzed.

Keywords External quantum efficiency, Internal quantum efficiency, Grain size, Grain boundaries recombination velocity, Columnar cylindrical grain

1. Introduction

In order to increase performance of the silicon solar cell, many characterization methods have been implemented. These methods are mostly based on determination of fill factor and conversion efficiency from the photocurrent-phototension (J_{ph}-V_{ph}) characteristic curve [1-3].

Among these, one noted the new approach used by Dionne et al. [4] for the carrier generation rate based on the power series method. This technique permitted to calculate the output power expressions and the fill factor (FF) as functions of grains size (g), grain boundaries recombination velocity (S_{gb}), illumination wavelength (λ), back side surface (S_b) and junction (S_f) recombination velocities.Authors showed that the output power and the fill factor (FF) decrease with increase of grain boundary recombination velocity and back surface recombination velocity for small grain sizes.

In another hand, Trabelsi et al. [5] evaluated the performance of a polycrystalline solar cell, covered at the backside by a quasi-monocrystalline porous silicon (SPQM). They showed with this technique that the photocurrent and the conversion efficiency increase of 4 mA.cm^{-2}and 2.25%, respectively. In addition, they concluded that the SPQM technique considerably improves the performance of thin solar cell with passivated grain boundaries.

It thus appears that the characteristic I-V curve makes it possible to obtain a lot of information on performances of solar cell, but it remains however limited [6-8]. It doesn't give any precise indication of location of losses and therefore the reason for the variation of one or several electrical parameters I_{cc}, V_{co} et FF [6-8]. The external quantum (EQE) and internal (IQE) efficiencies provide more information in this sense [6-12].

Extensive studies have also been carried out for a better improvement of the conversion efficiency by measuring the spectral response (SR) of crystallinesilicon solar cells, which makes it possible to evaluate the internal and external quantum efficiencies. For an example, the curve of the spectral response (SR) allows the determination of parameters such as the diffusion length whose high values correspond to a greater efficiency [6-12].

Thus, from determination of internal quantum efficiency (IQE), Madougou et al. [11]determined the recombination parameters of a bifacial silicon solar cell.When the cell is illuminated by its rear side, the experimental and theoretical internal quantum efficiencies increase with the wavelength range 0.4µm-0.97µmand then decreases thereafter. They showed that the diffusion length is lower for a wavelength range between 0.675µm and 0.95µm.

In the same sense, several authors [6-9, 12] also evaluated performance of solar cell through spectral response or internal quantum efficiency. However they have not investigated the external quantum efficiency. In order to obtain results that are closer to reality, some of these studies have taken into account influences of grain size and grain boundary recombination velocity through a three-dimensional model. It is the columnar cubic grain model that has been adopted to do these studies [6].

In this work, the cylindrical columnar grain model is used for characterization of an n^+/p polycrystalline silicon solar cell under monochromatic illumination in steady state operating condition. From this model, Bessel function and the dynamic junction velocity (S_f) corresponding to the junction recombination velocity in a recent past [2] are used to obtain in short-circuit operating mode, the expression of excess minority carriers density depending on the radius (R) and the depth (z) at a position in the base of the columnar cylindrical grain. Short-circuit photocurrent density (J_{SC}) and the quantum efficiencies (EQE and IQE) are also determined. The effects of the grain size corresponding to the grain radius (R) and the grain boundary recombination velocity (S_{gb}) on the external and internal quantum efficiencies of the solar cell are studied.

2. Model and assumptions

2.1. Analytical formulation

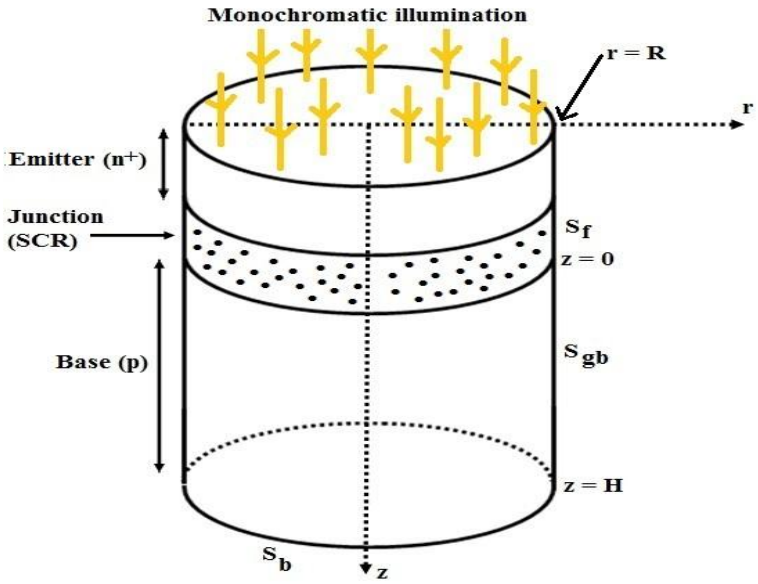

Figure 1: Isolated cylindrical columnar grain of a polycrystalline N^+/P solar cell

In this work, we propose a three-dimensional (3D) study of a polycrystalline silicon solar cell (n^+/p) operating under monochromatic illumination. The polycrystalline silicon solar cell is made up of several grains with different sizes and forms separated by grain boundaries [2-4, 6, 9, 13] which are recombination centers. For this study we use the cylindrical columnar grain model of an (n^+/p) polycrystalline solar cell. Each grain is supposed

to be a cylinder of thickness H and radius R as shown figure **(1)**.The variation of R corresponds to the variation of the grain size. The grain boundary corresponding to the lateral surface of the grain is located at r = R where recombination velocity (S_{gb}) is supposed to be constant.

2.2. Determination and resolution of the continuity equation

For the determination of the continuity equation of minority carriers (electrons), the following assumptions have also been taken into account:

- the intra-grain material is homogeneous and this leads to azimuthal symmetry. As a result, the number of independent coordinates are reduced to two, namely r and z, using the cylindrical coordinate system [2, 3, 9];
- we work in the theory of quasi-neutral basis (QNB) [2-4, 6, 13, 14];
- the contribution of the emitter is not taken into account as in[2-4, 13, 14];
- we work in low injection conditions.

On the basis of the above assumptions, the continuity equation of minority carriers in the base of the solar cell, in steady state and under monochromatic illumination is given by equation 1 [2, 3, 9]:

$$\frac{\partial^2\delta(\mathrm{r,z})}{\partial r^2}+\frac{\partial^2\delta(\mathrm{r,z})}{\partial z^2}+\frac{1}{r}\frac{\partial\delta(\mathrm{r,z})}{\partial r}-\frac{1}{L^2}\delta(\mathrm{r,z})=-\frac{G(\mathrm{z})}{D} \quad \textbf{(1)}$$

δ(r, z) is the excess minority carriers density in base of the solar cell; D and Lrepresent the coefficient and the diffusion length, respectively; G (z) is the electron-hole pairs generation rate [2, 3, 9]:

$$G(\mathrm{z})=\alpha\,\mathrm{I}_0(1-R')\exp(-\alpha z) \quad \textbf{(2)}$$

Equation 1 is a partial derivative differential equation for which the general expression of the solution can be written by equation3as[2, 3, 9]:

$$\delta(\mathrm{r,z})=\sum_{k\geq1}^{\infty}f_k(\mathrm{r}).\sin(\mathrm{C}_k.\mathrm{z})+\mathrm{K}_k \quad \textbf{(3)}$$

Using the orthogonality of the sinus function [2, 3, 9] and introducing Bessel functions, carrier's density expression is determined by equation (4):

$$\delta(r,\mathrm{z})=\sum_{k\geq1}^{\infty}\left[\begin{array}{l}A_k.r+\dfrac{2G_0}{HD(\mathrm{T})}\dfrac{L_k^2C_k}{C_k^2+\alpha^2}(1+(-1)^{k+1}\exp^{-\alpha H})\\ -\dfrac{2L_k^2K_k}{L^2H}\dfrac{1-\cos(C_k\,\mathrm{H})}{C_k}\end{array}\right]\sin(C_k.z)+\mathrm{K}_k \quad \textbf{(4)}$$

With: $L_k=\left(\frac{1}{L^2}+C_k^2\right)^{-\frac{1}{2}}$

The coefficients A_k, K_k and C_k are determined through following boundary conditions:

- at the junction (z=0) [2, 3, 9]:

$$\left.\frac{\partial\delta(r,z)}{\partial z}\right|_{z=0}=\frac{S_f}{D}\delta(\mathrm{r},0) \quad \textbf{(5)}$$

S_f represents the dynamic junction recombination velocity [1-4, 6, 11, 13, 14] and is imposed by the external load (S_{fj}) and losses at the junction (S_{f0}).

- at grain boundary (r=R) [2, 3, 9]:

$$\left.\frac{\partial\delta(r,z)}{\partial r}\right|_{r=R}=-\frac{S_{gb}}{D}\delta(R,\mathrm{z}) \quad \textbf{(6)}$$

where S_{gb} is the grain boundary recombination velocity .

- at back side surface of the solar cell (z=H) [2, 3, 9]:

$$\left.\frac{\partial\delta(r,z)}{\partial z}\right|_{z=H} = -\frac{S_b}{D}\delta(r,H) \quad \textbf{(7)}$$

with S_b corresponding to the back side recombination velocity.

By injecting the expressions of coefficients A_k, K_k and C_k into equation 4 and assuming that the solar cell is in short-circuit operating mode ($S_f \to +\infty$), the expression of carriers density in short-circuit is obtained, as shown in equation (8) :

$$\delta_{sc}(\mathrm{r,z}) = \sum_{k\geq 1} -\frac{2G_0L^2C_k}{D^2(C_k^2+\alpha^2)}\left\{1+(-1)^{k+1}\exp^{-\alpha H}\right\}\left[\frac{L_k^2 r}{L^2H(\frac{1}{S_{gb}}-\frac{R}{D})}-\frac{D}{H}\right]\sin(C_k z) \quad \textbf{(8)}$$

The expression of the short-circuit photocurrent density is then given by equation (9):

$$J_{SC} = qD\left.\frac{\partial\delta_{SC}(\mathrm{r,z})}{\partial z}\right|_{z=0} \quad \textbf{(9)}$$

2.3. Quantum efficiency

Its represents the ratio of the number of collected carriers in short-circuit operating condition by the number of incident photons for a given wavelength. Its expression is given by the equation 10 below [15]:

$$EQE(\lambda,\mathrm{r,Sgb}) = \frac{h.c.J_{SC}}{q.\lambda.I_0(\lambda)} \quad \textbf{(10)}$$

To study internal mechanisms in the solar cell, it is necessary to consider only the absorbed photons. The photons reflected or transmitted, as well as those absorbed in the non-active layers, are then separated from the calculation. Thus internal quantum efficiency (IQE) represents the ratio of short-circuit photocurrent density by the number of photons that have really been absorbed into the cell. Its expression is given by equation 11 [6, 15]:

$$IQE(\lambda,\mathrm{r,Sgb}) = \frac{EQE}{1-\Re'(\lambda)} \quad \textbf{(11)}$$

In these equations h, c, λ, q and $I_o(\lambda)$ represent the Planck constant, the velocity of light, the wavelength of exciter light, the elementary charge and the spectral irradiance, respectively.

3. Results and discussions

3.1. Effects of grain radius and grain boundary recombination velocity on the external quantum efficiency (EQE)

We plotted in figures 2 and 3 the curves of the external quantum efficiency versus wavelength for differents values of grain radius and grain boundary recombinaison velocity, respectively.

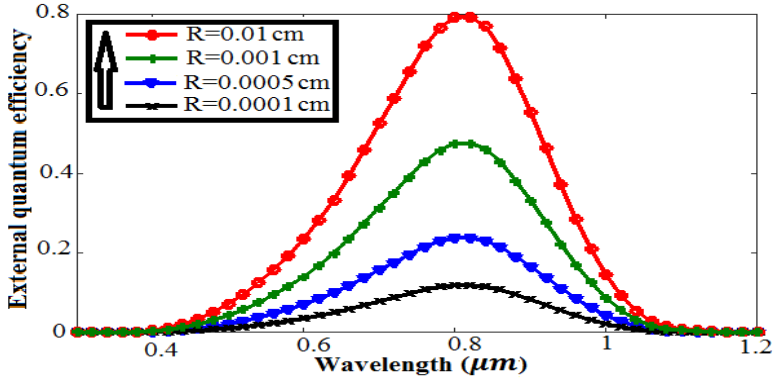

Figure 2:wavelength effect onexternal quantum efficiencyfor various grain size ($D=26cm^2.s^{-1}$, $S_b=10^3\ cm.s^{-1}$, $L=0.01\ cm$, $H=130\ \mu m$,$S_{gb}=2.10^2 cm.s^{-1}$).

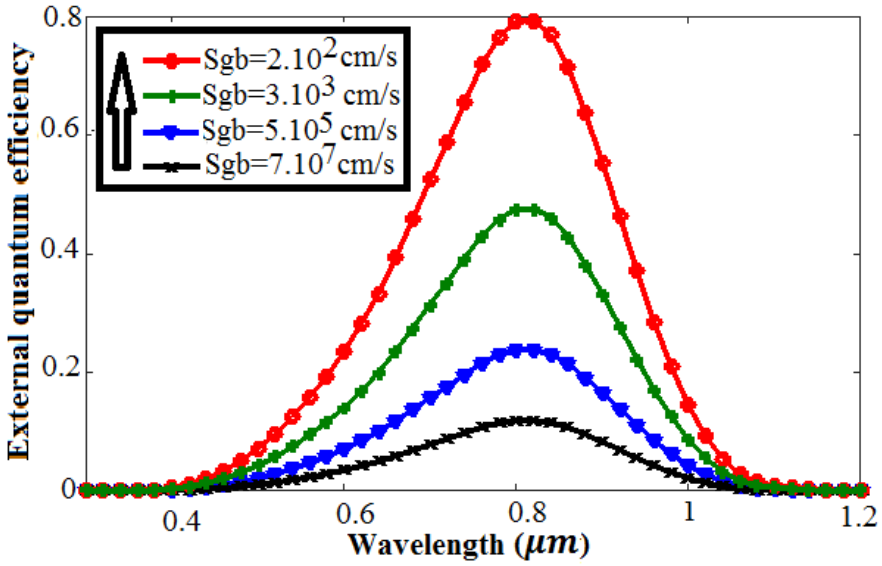

Figure 3: wavelength effect on external quantum efficiencyfor various grain boundary recombination velocity ($D=26cm^2.s^{-1}$, $S_b=10^3$ $cm.s^{-1}$, L=0.01 cm, H=130 µm, R=0.01 cm).

The external quantum efficiency curves of above figures 2 and 3 have been plotted for wavelengths ranging from ultraviolet (0.2 µm) to infrared (1.2 µm).

For a given grain radius and for a given grain boundary recombination velocity, the external quantum efficiency is practically null for wavelengths $\lambda \leq 0.4$ µm. Then its value increases with wavelength and reaches a maximum at$\lambda = 0.8$ µm. For the wavelengths $\lambda \geq 0.8$ µm, the external quantum efficiency decreases and become null when $\lambda \geq 1.1$ µm.

- When $\lambda \leq 0.4$ µm and $\lambda \geq 1.1$ µm, the external quantum efficiency is practically null: this means that there is no electrons collected through the external charge and then the short-circuit photocurrent density is null. This is related to the fact that photovoltaic conversion takes place only between 0.4 µm and 1.1 µm for silicon [14].
- For $0.4\ \mu m \leq \lambda \leq 0.8\ \mu m$, the variations of external quantum efficiency are mainly related to recombinations on front surface. For these wavelengths, the phenomenon of thermalization occurs, which is harmful for the cell. Indeed, for a photon energy greater than energy gap, excess energy contributes to increase the temperature, which leads to a decrease of performance [3, 16].The low values of external quantum yield can also be explained by reflexivity on the front of solar cell [8].
- For $0.8\ \mu m \leq \lambda \leq 1.1\ \mu m$, the variations of external quantum efficiency are related to important rear surface recombinations. Also because of short diffusion length of the carriers, they have very little chance to reach the junction and participate in photocurrent. This drop of external quantum efficiency is also related to low absorption for larges wavelength [8].

It appears from figure 2 that increase of grain radius leads to the increase of external quantum efficiency. As grain radius increases, the volume of the illuminated material increases. It resultsto an increase of the number of photogenerated carriers as well as the number of electrons collected through external charge.

Figure 3 shows that increase of grain boundary recombination velocity leads to a decrease of external quantum efficiency. When grain boundary recombination velocity increases, thecarriers density in the base decreases as the number of carriers collected through the external charge.

3.2. Effects of grain radius and grain boundary recombination velocity on the internal quantum efficiency (IQE)

We plotted in figures 4 and 5 the curve of internal quantum efficiency versus wavelength respectively for different values of grain radius and grain boundary recombinaison velocity.

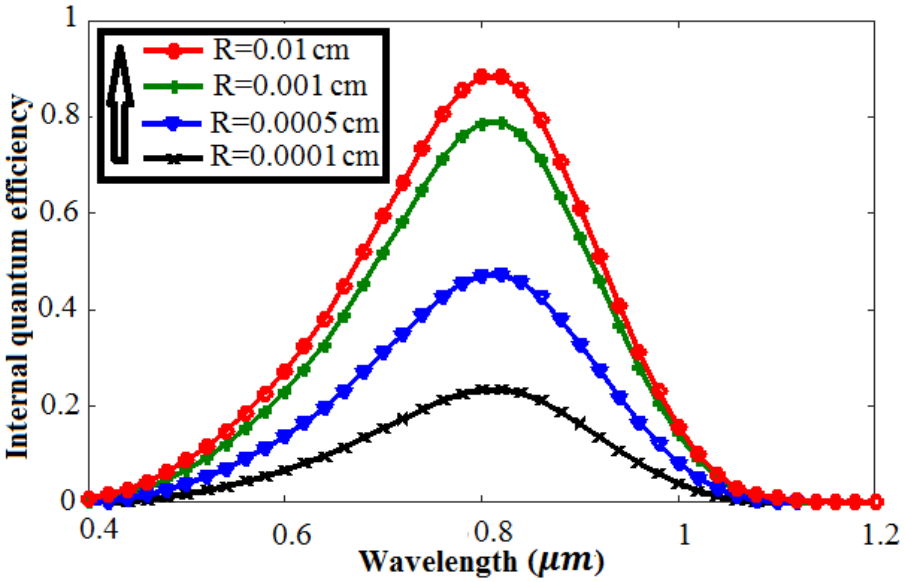

Figure 4: wavelength effect on internal quantum efficiency for various grain size ($D=26cm^2.s^{-1}$, $S_b=10^3$ $cm.s^{-1}$, $L=0.01$ cm, $H=130$ μm, $S_{gb}=2.10^2 cm.s^{-1}$).

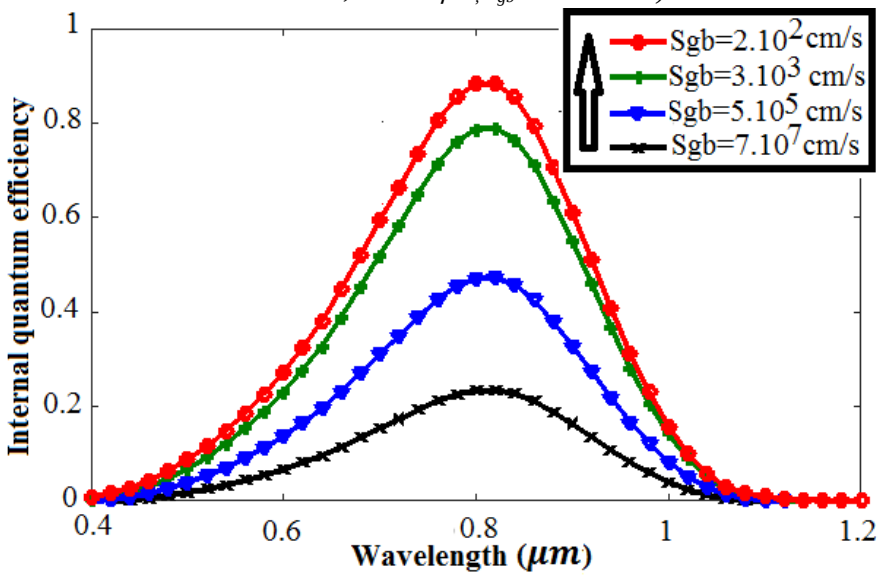

Figure 5: wavelength effect on internal quantum efficiency for various grain boundary recombination velocity ($D=26cm^2.s^{-1}$, $S_b=10^3$ $cm.s^{-1}$, $L=0.01$ cm, $H=130$ μm, $R=0.01$ cm).

In comparison with figures 2 and 3, the curves of figures 4 and 5 show that external and internal quantum efficiencies have the same profile. However, the internal quantum efficiency (IQE) has significantly larger values compared to external quantum efficiency (EQE).

The results shows that for grain radius R = 0.01 cm and grain boundary recombination velocity $S_{gb} = 2.10^2$ $cm.s^{-1}$, the maximum of external quantum efficiency is 80.00%while that of internal quantum efficiency is 88.31%.This result reflects importance of unabsorbed photons that represent reflected photons and those are transmitted. It also shows that it is more appropriate to use internal quantum efficiency to interpret losses inside solar cell.

- For 0.4 μm ≤ λ ≤ 0.8 μm, the variations of internal quantum efficiency are related to front surface recombination but also to phenomenon of thermalization. As the wavelength increases, these effects decrease and therefore the internal quantum efficiency increases to its maximum;

- For 0.8μm ≤ λ ≤ 1.1 μm, variations of internal quantum efficiency are related to effects of rear surface recombination and short diffusion length of carriers. As the wavelength increases, these effects increase and the internal quantum efficiency decreases.

Figure 4 shows that an increase of grain radius leads to an increase of internal quantum efficiency. Indeed, increasing grain radius lead to an increase of the volume of the illuminated material; corresponding to increase of carriers' generation and their collection through the external load as show with the columnar cubic grain model [6].

Figure 5 shows that an increase of grain boundary recombination velocity leads to a decrease of internal quantum efficiency. Indeed, by increasing grain boundary recombination velocity, carrier losses at grains boundaries also increase. This increase of carrier losses leads to a decrease of carriers' density in the baseas does the number of carriers collected through the external charge. These results are in perfect agreement with those of the columnar cubic model [6].

4. Conclusion

On the basis of cylindrical grain model, the continuity equation of minority carriers has been solved in cylindrical coordinates. In short-circuit situation, expressions of carrier density and photocurrent density were determined. Variations of external and internal quantum efficiency were plotted for different values of grain radius and grain boundary recombination velocity. The results show that internal quantum efficiency has significantly higher values relative to external quantum efficiency because of important reflections and transmissions of incident light. It appears that an increase of grain size, which is represented by grain radius, leads to an increase of quantum efficiency and beyond an increase of carriers collection. However, an increase of grain boundary recombination velocity leads to a decrease of quantum efficiency and thus a decrease of carriers collection.

References

[1]. G. Sissoko and S. Mbodji (2011). A Method to Determine the Solar Cell Resistances from Single I-V Characteristic Curve Considering the Junction Recombination Velocity (S_f),International Journal of Pure and Applied Sciences and Technology, 6(2), pp. 103-114.

[2]. A. Diouf, A. Diao, S. Mbodji (2018). Effect of the grain radius on the electrical parameters of an n+/p polycrystalline silicon solar cell under monochromatic illumination considering the cylindrical orientation,Journal of Scientific and Engineering Research, 5(2), pp. 174-180.

[3]. S. N. Leye, I. Fall, S. Mbodji, P. L. T. Sow, G. Sissoko (2018). Analysis of T-Coefficients Using the Columnar Cylindrical Orientation of Solar Cell Grain, Smart Grid and Renewable Energy, 9, 43-56.

[4]. M. M. Dione, A. Diao, M. Ndiaye, H. Ly Diallo, N. Thiam, F. I. Barro, M. Wade, A. S. Maiga, G. Sissoko (2010), 3D Study of a Monofacial Silicon Solar Cell Under Constant Monochromatic Light: Influence of Grain Size, Grain Boundary Recombination Velocity, Illumination Wavelength, Back Surface and Junction Recombination Velocities,25th European Photovoltaic Solar Energy Conference and Exhibition, 5th World Conference on Photovoltaic Energy Conversion, 6-10 September, Valencia, Spain.

[5]. A. Trabelsi, M. Krichen, A. Zouari and A. Ben Arab (2008). Effect of quasi-monocrystalline porous silicon at the backside on the photovoltaic parameters of a polycrystalline silicon solar cell, Revue des Energies Renouvelables, 11(3), pp. 395 – 405.

[6]. B. Zouma, A. S. Maiga, M. Dieng, F. Zougmore G. Sissoko (2009). 3D Approach of Spectral Response for a Bifacial Silicon Solar Cell Under a Constant Magnetic Field, Global Journal of Pure and Applied Sciences, 15(1), pp. 117 – 124.

[7]. N. Benaouda, R. Aiouaz, M. Abersi (2007). Réponses spectrales et des caractéristiques I-V des cellules solaires au silicium, Revue des Energies Renouvelables ICRESD-07 Tlemcen 145–150.

[8]. Kuo-Hui Yang, Jaw-Yen Yang (2011). The analysis of light trapping and internal quantum efficiency of a solar cell with grating structure, Solar Energy, 85, 419-431.

[9]. S. Elnahwy and N. Adeeb (1988). Exact Analysis of a Three dimensional Cylindrical Model for a Polycrystalline Solar Cell, J. Appl Phys. ,64 (10), 15 November.

[10]. G. Rolland (1985). Etude des variations de rendement quantique interned'un détecteur CCD en fonction de la température, Revue de Physique Appliquée, 20 (9), pp.651-659.

[11]. S. Madougou, F. Made, F. S. Boukary, G. Sissoko (2007). Recombination Parameter Determination By Using Internal Quantum Efficiency (IQE) Data of Bifacial Silicon Solar Cell, Advanced Materials Research, 18(19), pp. 313-324.

[12]. L.J. Geerligs, P. Manshanden, I. Solheim, E.J. Ovrelid, A.N. Waernes (2006). Impact of Common Metallurgical Impurities on mc-Si Solar Cell Efficiency: P-Type Versus N-Type Doped Ingots, 21st European Photovoltaic Solar Energy Conference and Exhibition, 4-8 September 2006, Dresden, Germany.

[13]. M. Savadogo, M. Zoungrana, I. Zerbo, B. Soro, D. J. Bathiebo (2017). 3-D modeling of grains sizes effects on polycrystalline silicon solar cell under intense light illumination, Sylwan, 161(8).

[14]. A. Ouedraogo, V. D. B. Barandja, I. Zerbo, M. Zoungrana, E. W. Ramde, D. J. Bathiebo (2017). A theoretical study of radio wave attenuation through a polycrystalline silicon solar cell, Turk J Phys,41, 314-325.

[15]. A. Luque, S. Hegedus (2011). Handbook of Photovoltaic Science and Engineering, Wiley.

[16]. B. Soro, M. Zoungrana, I. Zerbo, M. Savadogo, D. J. Bathiebo (2017). 3-D Modeling of Temperature Effect on a Polycrystalline Silicon Solar Cell under Intense Light Illumination, Smart Grid and Renewable Energy, 8, 291-304.